Remote Sensing of Environment 115 (2011) 703–714

Contents lists available at ScienceDirect

Remote Sensing of Environment

journal homepage: www.elsevier.com/locate/rse

Three-dimensional canopy fuel loading predicted using upward and downward sensing LiDAR systems

Nicholas S. Skowronski [a,b,*], Kenneth L. Clark [a], Matthew Duveneck [c], John Hom [d]

[a] USDA Forest Service, Northern Research Station, Silas Little Experimental Forest, 501 Four Mile Rd., New Lisbon, NJ 08064, USA
[b] Department of Ecology, Evolution, and Natural Resources, Graduate Program in Ecology and Evolution, Rutgers University, 14 College Farm Rd., New Brunswick, NJ 08901, USA
[c] Department of Environmental Sciences and Management, Portland State University, P.O. Box 751, Portland, OR 97207, USA
[d] USDA Forest Service, Northern Research Station, 11 Campus Blvd., Newtown Square, PA 19073, USA

ARTICLE INFO

Article history:
Received 30 September 2009
Received in revised form 4 October 2010
Accepted 30 October 2010

Keywords:
Canopy bulk density
Fuel loading
Wildfire
LiDAR
Fuel Maps
New Jersey Pinelands

ABSTRACT

We calibrated upward sensing profiling and downward sensing scanning LiDAR systems to estimates of canopy fuel loading developed from field plots and allometric equations, and then used the LiDAR datasets to predict canopy bulk density (CBD) and crown fuel weight (CFW) in wildfire prone stands in the New Jersey Pinelands. LiDAR-derived height profiles were also generated in 1-m layers, and regressed on CBD estimates calculated for 1-m layers from field plots to predict three-dimensional canopy fuel loading. We then produced maps of canopy fuel metrics for three 9 km^2 forested areas in the Pinelands.

Correlations for standard LiDAR-derived parameters between the two LiDAR systems were all highly significant, with correlation coefficients ranging between 0.82 and 0.98. Stepwise linear regression models developed from the profiling LiDAR data predicted maximum CBD and CFW ($r^2 = 0.94$ and 0.92) better than those developed from the scanning LiDAR data ($r^2 = 0.83$ and 0.71, respectively). A single regression for the prediction of CBD at all canopy layers had r^2 values of 0.93 and 0.82 for the profiling and scanning datasets, respectively. Individual bin regressions for predicting CBD at each canopy height layer were also highly significant at most canopy heights, with r^2 values for each layer ranging between 0.36 and 0.89, and 0.44 and 0.99 for the profiling and scanning datasets, respectively. Relationships were poorest mid-canopy, where highest average values and highest variability in fuel loading occurred. Fit of data to Gaussian distributions of canopy height profiles facilitated a simpler expression of these parameters for analysis and mapping purposes, with overall r^2 values of 0.86 and 0.92 for the profiling and scanning LiDAR datasets, respectively. Our research demonstrates that LiDAR data can be used to generate accurate, three-dimensional representations of canopy structure and fuel loading at high spatial resolution by linking 1-m return height profiles to biometric estimates from field plots.

Published by Elsevier Inc.

1. Introduction

Wildland fire managers have a strong interest in accurately mapping the structural characteristics of forest canopies. Maps of canopy fuel loading can be used to predict fire behavior and guide operational responses during active fire suppression, to prioritize areas for hazardous fuel reduction treatments, and to evaluate the effects of past fires or other disturbances. Thus, maximizing the accuracy of canopy fuel maps is vital to guiding the effective allocation of resources by fire management agencies. Fire behavior models such as NEXUS (Scott, 1999), FARSITE (Finney, 2004), and CFIS (Alexander et al., 2006) all use a generalized metric, termed canopy bulk density (CBD), to characterize canopy fuels. CBD is a measure of the mass of foliage and small branch wood that is available for combustion per unit volume within a forest stand (kg m^{-3} of combustible foliage and twigs; van Wagner, 1977). A second associated variable is total canopy fuel weight (CFW), defined as the total fuel that could be consumed within the canopy per unit ground area (kg m^{-2}).

Typically, CBD and CFW are measured using destructive harvesting techniques at the plot level. Data are then used to develop species-specific regression models to predict CBD and CFW from standard forest biometric measurements such as tree density, mean height, and diameter at breast height (DBH; diameter at 1.37 m) (Duveneck and Patterson, 2007; Keane et al., 1998, 2000). These biometric models can then be used to estimate CBD and CFW across larger areas using plot-based datasets such as USDA Forest Inventory and Analysis data (http://fia.fs.fed.us/). Optical and other indirect estimation methods have also been used to estimate canopy fuels at the plot level (Keane et al., 2005). While these estimation techniques have proven effective for the prediction of canopy fuels and crown fire potential at the scale of individual stands and in larger homogeneous management units, it is difficult to estimate crown fuels accurately across uneven aged,

* Corresponding author. USDA Forest Service, Northern Research Station, Silas Little Experimental Forest, 501 Four Mile Rd., New Lisbon, NJ 08064, USA.
E-mail address: nskowronski@fs.fed.us (N.S. Skowronski).

0034-4257/$ – see front matter. Published by Elsevier Inc.
doi:10.1016/j.rse.2010.10.012

disturbed, or otherwise heterogeneous forested landscapes. However, accurate mapping of these variables across landscapes characterized by heterogeneous canopy structure (both horizontally and vertically) and variable fuel loadings is important because fire behavior will tend to be much more dynamic and unpredictable.

With recent advances in Light Detection and Ranging (LiDAR) applications, a number of studies have demonstrated the potential use of LiDAR technology to generate landscape-scale maps of CBD, CFW and other canopy fuel parameters (Andersen et al., 2005; Clark et al., 2009; Riaño et al., 2004; Skowronski et al., 2007). Much of this work utilized standard LiDAR parameters such as maximum return height, average return height, percent cover, and decile height distributions, combined with data from forest biometric plots to develop regression models to predict canopy fuels (Andersen et al., 2005; Skowronski et al., 2007). LiDAR-derived parameters also have been used in the assignment of fire behavior models (e.g., Scott and Burgan, 2005) based on the fusion of LiDAR and reflectance data (Mutlu et al., 2008). In addition, LiDAR-derived canopy height profiles (CHPs), which provide structural data in 1-m layers, have been used to characterize the three-dimensional distribution of biomass and fuel loading parameters through the forest canopy using full-waveform LIDAR (Parker et al., 2004a), downward sensing discrete-return profiling data (Skowronski et al., 2007), and discrete-return scanning LIDAR data (Popescu and Zhao, 2008).

An important next step in the generation of accurate three-dimensional representations of canopy fuel loading across forested landscapes is linking LiDAR-derived return height profiles with field biometric measurements to generate high-resolution profiles of CBD at discrete canopy heights. Representations of canopy fuel loading in a three-dimensional grid space would considerably expand upon our current use of two-dimensional canopy fuel characteristics such as CBD_{max} and CFW. In one approach, Stoker (2009) discussed the use of voxels as a potential way to characterize forest fuels in three dimensions using LiDAR data. This more accurate assessment of canopy fuel structure facilitates the development and parameterization of more complex fire spread models. For example, the Wildland-urban interface Fire Dynamics Simulator (WFDS) is now able to simulate fire spread through individual trees and shrubs with horizontal and vertical resolutions as fine as 8.5 cm (Mell et al., 2006).

Our study focuses on the ability of two independent LiDAR systems to assess canopy fuel characteristics in pitch pine (*Pinus rigida* Mill.)-dominated stands that are prone to wildfires in the Pinelands of New Jersey. We first developed allometric estimates of canopy bulk density and crown fuel weight in 24 field plots where we measured all trees. We calculated CBD and CFW using a model developed from harvesting of pitch pine by Duveneck and Patterson (2007) to predict these variables. We then calibrated two commonly used LiDAR systems, an upward sensing profiling system and a downward sensing scanning system, to these field plots. While the use of scanning LiDAR to estimate canopy fuels allows large-spatial scale estimates and landscape level maps of canopy fuels, the more mobile and less expensive upward sensing profiling LiDAR system can provide immediate canopy fuel estimates. We used three approaches to calibrate the LiDAR systems in these stands; 1) we developed regression equations between standard LiDAR return parameters and biometric estimates of CBD and CFW derived from the field plots, 2) we developed regressions between LiDAR CHPs and biometrically derived canopy bulk density profiles to predict canopy fuels at 1-m intervals through the canopy, and 3) we fit Gaussian distributions to the LiDAR-derived CHPs and to the biometric CBD profiles, and evaluated the ability of these three-parameter algorithms to condense the information involved in the mapping of three-dimensional canopy fuels. We then explored the utility of these three approaches to characterize and visualize canopy fuel loads in pitch pine–scrub oak stands in the Pine Barrens of New Jersey.

2. Methods

2.1. Study area

Study sites are located in Ocean and Burlington Counties in the Pinelands National Reserve (hereafter, Pinelands) of southern New Jersey. The Pinelands encompass ca. 400,000 ha of pine and oak-dominated upland forests, and various wetland forest types. Upland forests comprise 62% of forested land. Stands are dominated by pitch pine, shortleaf pine (*Pinus echinata* Mill.), and various oaks (*Quercus* spp.) in three major communities; oak-dominated communities with scattered pines (Oak–pine, 46% of upland forests), pine-dominated forests with oaks in the overstory (Pine–oak, 31% of upland forests), and pitch pine-dominated forests with scrub oak and shrubs in the understory (Pine–scrub oak, 23% of upland forests) (Clark et al., 2009; Lathrop and Kaplan, 2004; McCormick and Jones, 1973; Skowronski et al., 2007). All upland forests have moderate to dense shrub cover in the understory, primarily *Vaccinium* spp., *Galussacia* spp., *Kalmia* spp., and *Quercus* spp. (Wright et al., 2007). Various sedges, mosses and lichens are also present.

2.2. Field methods

2.2.1. Field plots and biometric measurements

We conducted our field sampling within three scanning LiDAR acquisitions, each measuring 9 km^2 (Fig. 1). Within each 9 km^2 acquisition, the 2001 NJ Land-Use/Land Change map (Lathrop and Kaplan, 2004) was used to delimit stands consisting of >75% pitch pine overstory in pitch pine–scrub oak stands. Field plot locations were generated using random UTM coordinates, and were in stands that were at least 4 ha in size, buffered by a minimum of 100 m from the edge of the stand, and at least 100 m apart from each other. Using these criteria, we established 24 20 × 20 m plots. The UTM coordinates of the plot corners were recorded using a high-accuracy, differentially corrected GPS (Pathfinder ProXT, Model # 52240-20, Trimble Navigation Limited, Sunnyville, CA) in order to accurately georeference the scanning LiDAR point clouds to the plot locations. Positional accuracy was recorded at sub-m precision, and when differentially corrected, had a mean reported standard deviation of 0.4 m for 96 recorded points (24 plots with 4 corners per plot). We then recorded species and crown class (dominant, co-dominant, intermediate, or suppressed), and measured diameter at breast height (DBH) and tree height using a Hypsometer (Haglof VL400, Haglof Sweden AB, Langsele, Sweden) for each tree >2 m height (the height at which they would be detected by the upward-looking LiDAR sensor) in each plot.

We focused our field sampling efforts on the 9 km^2 acquisition around the Cedar Bridge fire tower in Greenwood Wildlife Management Area in the Pinelands (Fig. 2). The upper right corner of the image indicates the location of a 8,000 ha wildfire that occurred in 1995, and areas where crowning occurred are denoted with blue cross-hatch. The area in the light green strip running north to south near the center of the image is managed as a fuel break, and prescribed fires are conducted every 2–3 years (Fig. 2).

2.2.2. Upward sensing profiling LiDAR measurements

We used an upward sensing, profiling LiDAR system mounted on a backpack frame to collect data in each field plot. The instrumentation consisted of a discrete-return Riegl Laser Rangefinder (Model # LD90-3100VHS-FLP, Riegl USA, Orlando, FL), with a range of 0.1–200 m, connected to a PDA which collected first returns at 100 Hz via the RS-232 port. Spot size for this instrument ranges from 12.4 cm^2 at 1 m to 25.6 cm^2 at 50 m (Parker et al., 2004b). The instrument was paced at a constant rate along 20 north–south oriented transects spaced 1 m apart within each plot. Sky shots (laser pulses that passed through the canopy) were recorded as null values. Data below 2 m were not collected because the LiDAR instrument was mounted in the backpack

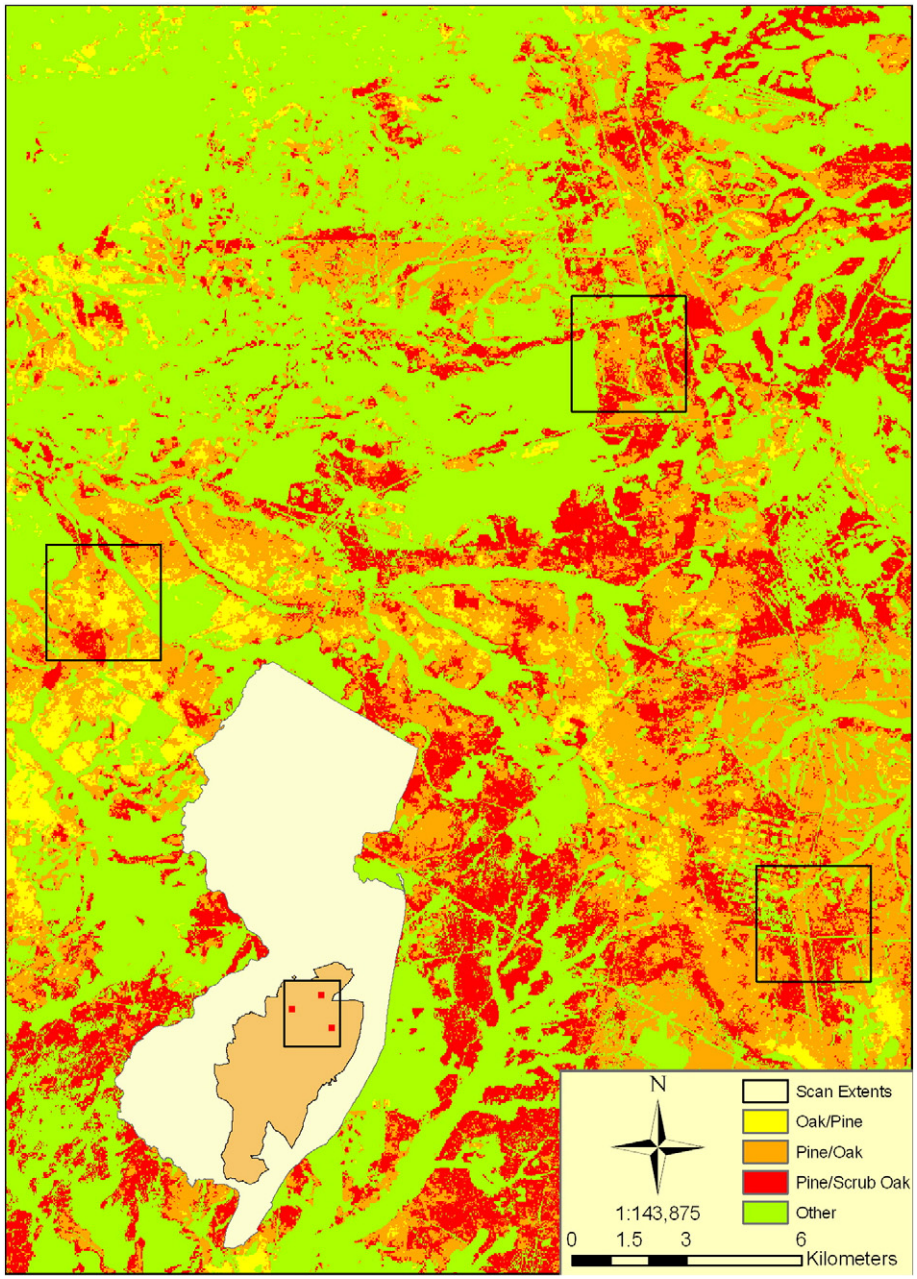

Fig. 1. Study sites in the Pinelands National Reserve, southern New Jersey. The inset shows the Pinelands National Reserve and black lines denote the location of the three 9-km^2 scanning LiDAR acquisitions intensive study areas where overlapping LiDAR data were collected. The larger map indicates the major upland forest types (adapted from Lathrop and Kaplan, 2004; Skowronski et al., 2007).

at approximately 2 m above the ground. We recorded an average of 2007 ± 516 pulses (mean $\pm$ 1 SD) per each 20 m line, for a total of $40{,}140 \pm 10{,}328$ pulses for each field plot.

2.2.3. Downward sensing scanning LiDAR measurements

A multiple return scanning LiDAR system (Optech ALTM 2025/2050, Optech Incorporated, Vaughn, Ontario) was flown over the three 9 km^2 study areas via fixed-wing aircraft on June 9, 2006 during leaf-on conditions by Airborne 1 Corp. (El Segundo, CA). The spot size for this instrument was ca. 95 cm^2 based on the manufacturer's specifications. These data had an average spacing of ca. 4 pulses m^{-2}, resulting in 704 ± 259 pulses for each 20 by 20 m plot. Between one and four returns were associated with each laser pulse, but only first returns were used for analyses, facilitating direct comparison with the profiling LiDAR sensor which recorded only first returns.

2.3. Data analyses

2.3.1. Field plots and biometric measurements

Canopy fuel parameters were calculated for each field plot using allometric equations for pitch pine derived from Duveneck and Patterson (2007). They used destructive harvests of trees ranging from 2.7 to 42.5 cm DBH and 4.1 to 23.8 m height in Montague, MA, and Martha's Vineyard, MA, to develop allometric equations to predict CFW, and then derived equations to calculate a profile of the distribution of canopy bulk density through the canopy. Their CBD_{bin} distribution was calculated using a 3-m running mean of canopy fuel to estimate CBD_{bin} in 1-m layers for each tree (Scott and Reinhardt, 2001). We used their CBD calculator (http://www.umass.edu/nebarrensfuels/methods/index.html) to estimate CFW and CBD_{bin} in 1 m layers for all trees measured in each field plot, and summed data for all trees to develop whole-plot estimates of

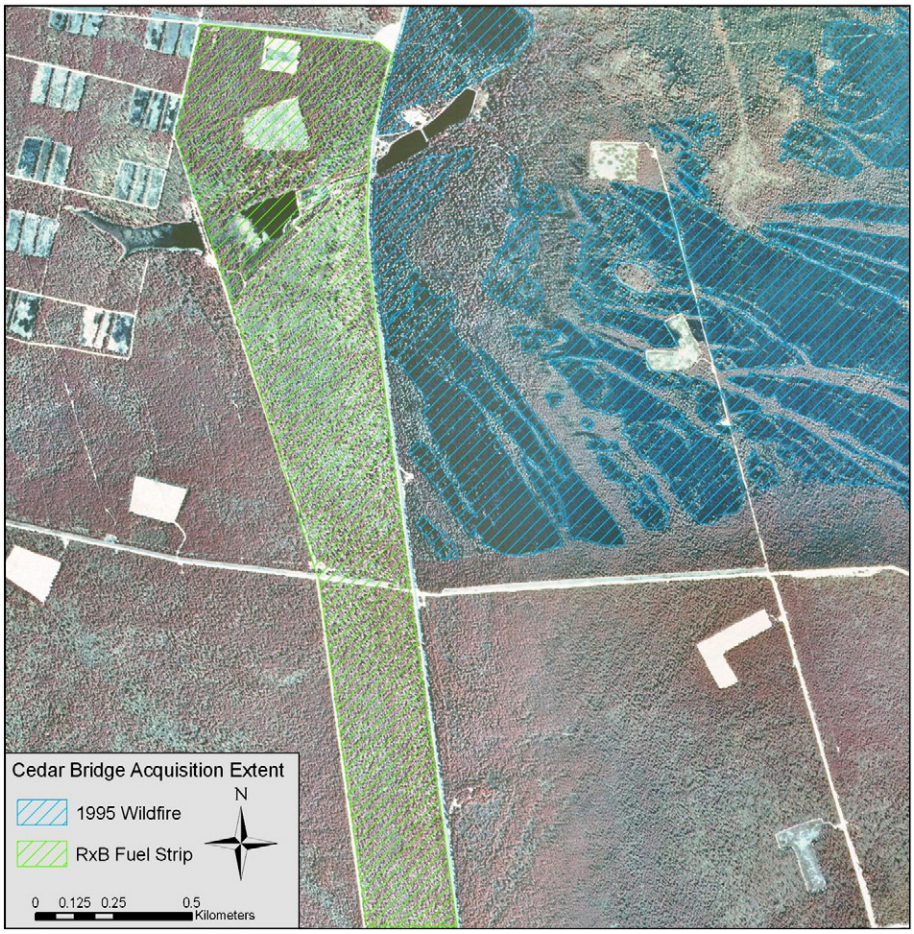

Fig. 2. Digital orthophoto of the 9 km^2 LiDAR acquisition near the Cedar Bridge fire tower taken immediately following the 1995 wildfire. Areas where crowning wildfire occurred are depicted by blue cross-hatch in the upper right, and the area burned every 2–3 years using prescribed fires is shown as green cross-hatch from north to south in the center of the image.

CFW and CBD_{bin}. CBD_{max} was calculated as the maximum mean 1 m CBD_{bin} value in each plot.

2.3.2. LiDAR datasets

Standard LiDAR parameters were calculated from the profiling LiDAR data for each plot, including maximum return height (h_{max}), average return height (h_{mean}), decile height values (h_{10}, h_{25}, h_{75}, and h_{90}), canopy cover (non-sky returns/all returns, D), and coefficient of variation (CV). All returns from the scanning LiDAR dataset were used to derive ground using a simple minimum grid technique, which has been determined to adequately characterize relatively flat terrain with ±1% error when compared to USGS 1:24,000 DEMs (USGS, EROS Data Center). Returns were attributed as either zero for ground returns, or as height above the ground for all other returns. Standard LiDAR parameters were then calculated for each plot. Scanning LiDAR point clouds were only analyzed for 19 of the field census plots, because five plots fell outside of the scanning LiDAR acquisition.

LiDAR datasets were then processed using Eqs. (1) and (2) to estimate CHPs in 1-m layers, or bins (e.g., bin 3 is a 1 m thick volume of canopy between 3 and 4 m above ground level), analogous to percent cover in 1-m layers (Skowronski et al., 2007):

$$\text{Returns in height bin } n = R_n/R_{total} \quad (1)$$

$$\text{Returns in height bin } n+1 = R_{n+1}/(R_{total} - R_n) \quad (2)$$

where R_n is the number of returns in the first height bin, R_{total} is the total number of returns, and R_{n+1} is the number of returns from the next bin in the canopy. Thus, the transformation progressed upward through the canopy for the profiling LiDAR data, and downward through the canopy for the scanning LiDAR system. Scanning LiDAR data were processed using Merrick MARS© software (Version 5, Merrick and Company, Aurora, CO).

2.3.3. LiDAR data comparisons

The profiling and scanning LiDAR data were first compared to examine relationships between sensors for return heights and % cover estimates using correlation analyses (Pearson's Product moment). CHPs derived from Eqs. (1) and (2) for each system were then compared in two ways; data from each height bin for every plot was used in a single comparison, and one correlation coefficient was calculated for 19 plots × 20 height bins for a total $n = 380$ data points, and an "individual bin" comparison where correlation coefficients were calculated for each height bin. This method generated 20 individual 1-m height bin correlations, where $n = 19$ plots.

2.3.4. LiDAR-derived canopy fuel models

We developed equations to predict CBD_{max} and CFW using stepwise linear regression analyses in SYSTAT 12 (Systat Software, Inc., Chicago, IL) from standard LiDAR metrics calculated from the profiling and scanning datasets and the field plot data, following Andersen et al. (2005). We used these equations to produce maps of CBD_{max} and CFW for each 9 km^2 scanning LiDAR acquisition. We then developed regression equations to predict CBD_{bin} in 1 m thick layers from the LiDAR-derived CHPs and CBD_{bin} estimates from the field

plots. Data were analyzed in two ways; all height bins for every plot were pooled to produce a single regression equation to predict CBD_{bin}, and separate regression equations were developed to predict CBD_{bin} for each 1-m height bin. To evaluate potential model overfitting, we utilized the SIMPLS program in Systat 12, an iterative "leave-one-out" cross-validation algorithm, to calculate a PRESS statistic (Myers, 1990; Popescu et al., 2003). We used the root mean square of the PRESS statistic, analogous to the root mean square error of cross-validation ($RMSE_{cv}$), for comparison to the root mean square error (RMSE) calculated using the complete datasets. The resultant predictive models were used to produce maps of CBD_{bin} in 1-m layers for each 9 km^2 scanning LiDAR acquisition. We used two different color coding schemes to indicate values of CBD on each map. The first scheme used green for low CBD values, and red for high CBD values. The second color coding scheme used a three-band, red, green and blue (RGB) composite image to display three separate canopy layers (i.e., 3-m, 8-m, and 13-m), with color intensity reflecting relative CBD values.

2.3.5. Gaussian distributions

Because of the large amount of LiDAR data associated with calculating return height profiles at 1-m increments, we explored the use of distribution analyses to reduce computation times. In this approach, the entire CBD profile can be represented using only three parameters, and displayed spatially as a raster. Landscape patterns of CBD can then be visualized as a three-band red, green and blue (RGB) composite image, unlike the individual bin approach where only three discrete bins at a time can be visualized. We fit three-parameter Gaussian distributions to both the CBD profiles calculated from the field census plots and the CHP derived from LiDAR datasets:

$$f(x) = ae^{[-0.5((x-x0)/b)\hat{}2]} \quad (3)$$

where a = maximum value of the distribution, x_0 = locus of the maximum, and b = full-width at half maximum. These parameters were fit dynamically to both the biometrically derived model and the LiDAR-derived CHPs in Sigma Plot (Version 10, Systat Software Inc., Chicago, IL). Linear regression models were developed for each of the Gaussian distribution parameters (a, x_0, and b) for predicting CBD_{bin} from profiling and scanning LiDAR canopy height profiles. Models were evaluated using the "leave-one-out" approach described above.

3. Results

3.1. Field plots and biometric data

Average tree height was 9.7 ± 2.6 m (mean ± 1 SD), and ranged between 6.0 m and 14.1 m in the 24 plots (Table 1). Mean maximum canopy bulk density estimated using allometric equations was 0.09 kg m^{-3}, and ranged from 0.02 kg m^{-3} to 0.17 kg m^{-3}. Mean crown fuel weight was 2.2 kg m^{-2}, and ranged from 0.4 kg m^{-2} to 4.5 kg m^{-2} for the 24 field plots. Datasets with 24 and 19 plots had similar canopy metrics and canopy fuel parameters (Table 1).

3.2. LiDAR data comparisons

Standard LiDAR canopy parameters were highly correlated among the profiling and scanning LiDAR systems (Table 2; Figs. 3 and 4). For example, h_{mean}, h_{90}, h_{75}, h_{25}, and h_{10} all had correlation coefficients ≥0.9. However, slopes and intercepts differed in most cases (e.g., Fig. 3). The correlation coefficient calculated for the LiDAR-derived CHPs from all height bins and plots between LiDAR systems was 0.85 (Table 2). Correlation coefficients for individual height bin comparisons among sensors ranged between 0.38 at 3 m height and 0.92 at 12 m height (Table 2; Fig. 4).

Table 1
Stand and canopy structure in n = 24 and n = 19 field plots in pitch pine–scrub oak stands in the Pinelands of New Jersey. Maximum canopy bulk density (CBD_{max}) was calculated as the maximum CBD_{bin} value in a 1-m thick layer, and canopy fuel weight (CFW) was calculated from Duveneck and Patterson (2007). All values are plot means ± 1 SD.

Parameter	n = 24 plots	n = 19 plots
Stems ha^{-1}	1029 ± 900	1184 ± 893
DBH (cm)	17.59 ± 6.36	16.19 ± 5.95
Basal area (m^2 ha^{-1})	17.63 ± 8.19	19.23 ± 5.57
Mean tree height (m)	9.74 ± 2.56	9.62 ± 2.68
Maximum tree height (m)	13.20 ± 2.57	13.47 ± 2.31
Canopy bulk density (CBD_{max}, kg/m^3)	0.088 ± 0.040	0.097 ± 0.033
Canopy fuel weight (CFW, kg/m^2)	2.22 ± 1.04	2.42 ± 0.73
Canopy bulk density (CBD_{bin}, kg/m^3) at selected canopy heights		
3-m height	0.009 ± 0.007	0.010 ± 0.007
8-m height	0.072 ± 0.044	0.080 ± 0.042
13-m height	0.022 ± 0.034	0.021 ± 0.024

CFW, CBD_{bin} and CBD_{max} were estimated with predictive models presented by Duveneck and Patterson (2007) by using their calculator available at: http://www.umass.edu/nebarrensfuels/methods/index.html.

3.3. LiDAR-derived canopy fuel models

Best fit stepwise linear regression equations for predicting CBD_{max} and CFW using LIDAR data were based on height metrics (h_{mean}, h_{max}, h_{90}) and canopy cover (D), and were highly significant for both systems (Table 3). Equations that predicted CBD_{max} and CFW using the profiling LiDAR data had higher values for regression coefficients than those using the scanning LiDAR data. Close agreement of $RMSE_{cv}$ and RMSE statistics suggests that the models accurately predicted these two-dimensional canopy fuel variables without overfitting. Predicted values of CBD_{max} and CFW from upward profiling LiDAR data and the downward scanning LiDAR data are presented as a scatter plot against biometric estimates of CBD_{max} and CFW in Fig. 5.

Table 2
The relationship between LiDAR parameters derived from upward sensing profiling LiDAR to downward sensing scanning LiDAR for n = 19 20 m × 20 m plots. Means and standard deviations of the number of returns for each parameter are presented for each sensor, raw and uncorrected. Correlation coefficients (r^2) are Pearson's product-moments. Correlations are all significant at P<0.0001, except where * indicates a significant correlation at P<0.05.

Parameter	Profiling LiDAR	Scanning LiDAR	Equation	r^2
Standard LiDAR-derived parameters				
Mean return height, h_{mean}	6.54 ± 1.48	7.71 ± 1.66	$y = 0.735x + 0.940$	0.98
Maximum return height, h_{max}	12.04 ± 3.07	12.40 ± 2.29	$y = 1.288x - 3.599$	0.82
90th percentile height, h_{90}	8.85 ± 1.83	10.00 ± 2.00	$y = 0.746x + 1.451$	0.96
75th percentile height, h_{75}	7.80 ± 1.72	9.00 ± 1.88	$y = 0.692x + 1.652$	0.94
25th percentile height, h_{25}	5.51 ± 1.43	6.51 ± 1.54	$y = 0.662x + 1.276$	0.94
10th percentile height, h_{10}	4.41 ± 1.23	5.36 ± 1.31	$y = 0.713x + 0.640$	0.90
Canopy density, D(%)	44.5 ± 17.9	87.8 ± 9.61	$y = 1.262x - 62.1$	0.86
Coefficient of variation, CV	0.26 ± 0.03	0.24 ± 0.43	$y = 0.540x + 0.128$	0.67
Canopy height bins				
All height bins (n = 475)	0.04 ± 0.06	0.14 ± 0.19	$y = 0.320x - 0.001$	0.85
Selected 1-m height bins (n = 19 for each bin)				
3-m height	0.01 ± 0.01	0.05 ± 0.06	$y = 0.081x + 0.009$	0.38*
8-m height	0.16 ± 0.09	0.40 ± 0.20	$y = 0.398x - 0.016$	0.86
13-m height	0.03 ± 0.04	0.11 ± 0.11	$y = 0.224x - 0.001$	0.93
Gaussian distribution				
a	0.19 ± 0.09	0.46 ± 0.21	$y = 2.06x + 0.0747$	0.84
b	1.75 ± 0.33	2.17 ± 0.31	$y = 0.728x + 0.893$	0.61
x_0	7.79 ± 1.31	7.96 ± 1.35	$y = 0.892x + 1.006$	0.75
CHP_{bin}	0.04 ± 0.04	0.04 ± 0.03	$y = 0.94x + 0.011$	0.83

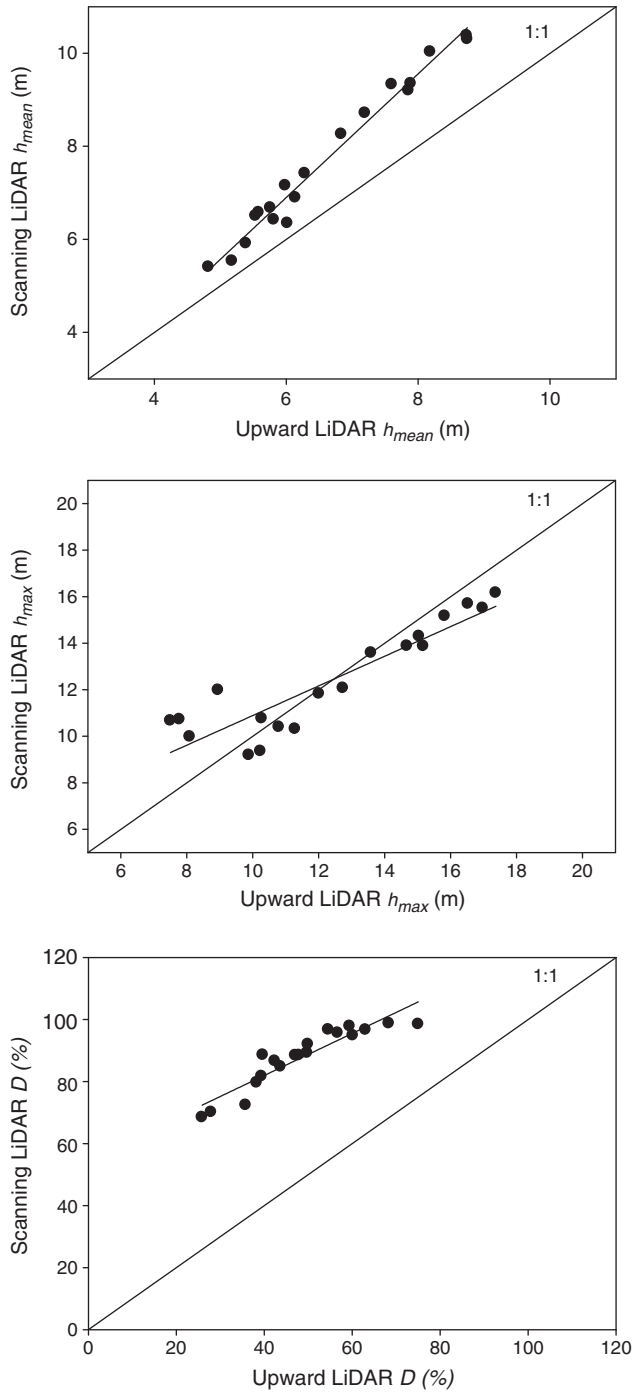

Fig. 3. Mean return height (h_{mean}) and mean maximum return height (h_{max}) in meters, and percent canopy cover (D) in co-registered plot locations ($n=19$) for upward scanning profiling and downward scanning LiDAR datasets.

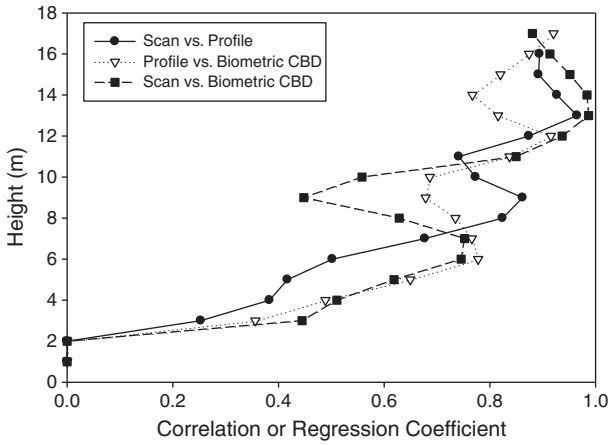

Fig. 4. Pearson's product moment correlation coefficients for the relationships between profiling LiDAR and scanning LiDAR return heights (m) in individual 1-m canopy height bins, regression coefficients for profiling LiDAR return heights and biometric estimates of canopy bulk density (CBD_{bin}) in 1-m canopy height bins, and regression coefficients for biometric estimates of CBD_{bin} and scanning LiDAR return heights in 1-m canopy height bins.

Predicted values of CBD_{max} at 20 by 20 m resolution for the 9 km^2 area at Cedar Bridge ranged from 0.0 to 0.232 kg m^{-3} (Fig. 6). Using scanning LiDAR data to predict a single value for CBD_{max} detected much of the spatial variability in CBD_{max}. Roads and open areas are obvious, and lower CBD values associated with wetland forest stands and pine–oak stands with a greater abundance of oaks also are apparent (shown as light green to yellow areas at the top and two bottom corners of Fig. 6). The prescribed fire strip in the middle of the image also has a lower overall CBD_{max} value, compared to the denser pitch pine scrub oak stands to the east and west of the strip (shown as orange and red areas to the left and right of the strip in Fig. 6). The dense pitch pine-dominated areas in the center of the image display large CBD values because of rapid resprouting following the 1995 wildfire.

Single regression models which used data for all plots and canopy heights to predict CBD_{bin} at discrete height bins had a regression coefficient of 0.83 for the profiling LiDAR system and 0.82 for the scanning LiDAR system (Table 4). The "individual bin" regression equations developed to predict CBD_{bin} were significant for both sensors, although the ability to predict CBD_{bin} differed among 1-m layers through the canopy (Table 4; Fig. 4). In Fig. 4, an increase in the value of the regression coefficients for both sensors occurs until 7 m height in the canopy, and then drops to a minima at approximately 9 m height. Regression coefficients then increase again to a second maxima at 14 and 12 m height for the profiling and scanning LiDAR data, respectively. The depression in the value of regression coefficients at 9–10 m height corresponds to mean canopy height in the field plots, but more importantly corresponds to the peak in variability of biometrically derived estimates of CBD_{bin} (Fig. 4).

When predicted values of CBD_{bin} derived from upward profiling LiDAR data or the downward scanning LiDAR data were plotted against biometric estimates of CBD_{bin}, values again scattered around the 1:1 line (Fig. 7). Estimated CBD_{bin} in 1-m layers at 20 m by 20 m resolution for the 9 km^2 area at Cedar Bridge derived from scanning LiDAR data is shown in Fig. 8, and demonstrates the ability of this approach to resolve complex canopy structure. Fig. 8a shows a "raster

Table 3
Best fit stepwise linear regressions for predicting maximum canopy bulk density (CBD_{max}, kg m^{-3}) and canopy fuel weight (CFW, kg m^{-2}) and using profiling and scanning LiDAR data. All regressions are significant at $P<0.001$.

LiDAR system	Model [a]	r^2	RMSE	$RMSE_{cv}$ [b]
Profiling LiDAR				
$CBD_{max} = -0.005\, h_{max} + 0.211\, D + 0.051$		0.94	0.010	0.012
$CFW = -0.049\, h_{max} + 5.587\, D + 0.33$		0.92	0.313	0.354
Scanning LiDAR				
$CBD_{max} = -0.008\, h_{max} - 0.001\, h_{mean} + 0.262\, D - 0.029$		0.77	0.017	0.019
$CFW = -0.129\, h_{90} + 6.368\, D - 1.877$		0.71	0.362	0.430

[a] h_{max}, maximum canopy height; h_{mean}, mean canopy height; D, percent cover (# of canopy returns/ total # of returns); h_{90} , height of 90th percentile.
[b] Square root of the mean of the PRESS statistic from leave-one-out cross-validation.

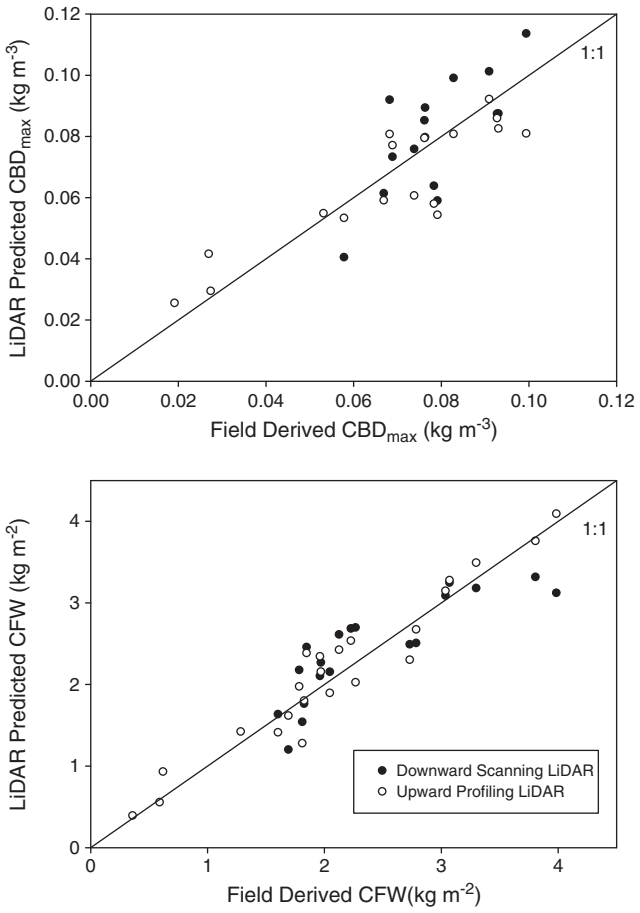

Fig. 5. Predicted values of CBD_{max} and CFW from equations for upward profiling LiDAR (open symbols) and downward scanning LiDAR systems (closed symbols) in Table 3 plotted against biometric estimates of CBD_{max} and CFW from field plots.

stack" of CBD_{bin} values for a 7-m thick canopy volume calculated from the scanning LiDAR data acquisition. In Fig. 8b–d, canopy bulk density at 3, 8 and 13 m heights indicate the spatial variability in CBD_{bin} values, again using green for low values and red for high values. Predicted CBD_{bin} at 3–4 m height in the prescribed burn strip running from north–south strip is relatively low, and values also are low in wetland forests and pine–oak stands where oaks are more abundant compared to pitch pine-dominated pine–scrub oak stands (shown in green and yellow from top to bottom at the center of the image, and at the top and in the lower right and left corners of the image in Fig. 8b). A dense band of high CBD values occurs from east to west near the center of the image, corresponding to areas burned intensely in the 1995 wildfire at the 3–4 m height level (shown in red to the left and right of the of the prescribed burn strip). However, at the 8–9 m height, lower CBD_{bin} values occur in the area of crowning wildfire. At the 13–14 m height, only the tallest canopies in scattered wetland forests in the upper portion of the image, and in stands containing a larger number of oaks in the lower right and left corners of the acquisition have relatively high CBD_{bin} values. This approach provides increased vertical resolution over the CBD_{max} values displayed in Fig. 6, allowing for increased understanding of where the highest amounts of fuels occur in the canopy profile.

Fig. 9 shows the CBD_{bin} at 3-m, 8-m and 13-m heights using the red, green and blue (RGB) color scheme, with color intensity reflecting relative CBD values. Differences and details that were not apparent in Fig. 6 are much more visible using this color additive scheme, illustrating the spatial complexity of the fuel loading and canopy structure in this area. Dense fuel loading at 3–4 m height is apparent in the upper right corner, reflecting the effects of the 1995 wildfire. At 8–9 m height, relatively dark green areas are apparent throughout the image, with the exception of the upper right corner where the 1995 wildfire burned. Only the tallest canopies in the wetlands (upper portion of the image) and the pine–oak stands in the two lower corners appear as dark blue in the image (Fig. 9).

3.4. Gaussian distributions

Relationships between the Gaussian distribution parameters from the profiling LiDAR and scanning LiDAR-derived CHPs were highly significant, with correlation coefficients of 0.84 for *a*, 0.61 for *b*, and 0.873 for x_0 (Table 2). The relationship between the profiling LiDAR and scanning LiDAR CHPs following the Gaussian transformation resulted in an r^2 of 0.83 (using individual height bins for comparison).

The fit of a Gaussian distribution to the biometrically derived CBD profiles, and to LiDAR-derived canopy height profiles for both profiling and scanning LiDAR data yielded highly significant correlation coefficients, ranging from 0.94 to 0.99 for individual plots. Regression models developed to predict *a*, *b*, and x_0 parameters of the biometrically derived CBD profiles from LiDAR CHPs were highly significant (Table 5). However, the profiling system was not able to predict the spread of this distribution (*b*) as well as the scanning system, with values of 0.489 and 0.798, respectively (Table 5). When these regression models were applied to the raw LiDAR CHPs, each sensor was able to predict the CBD_{bin} well, with correlation coefficients for the profiling and scanning LiDAR systems of 0.86 and 0.92, respectively (Table 5). A scatterplot of the field derived CBD_{bin} versus the LiDAR-derived (Gaussian transformed) CBD_{bin} is presented in Fig. 10. The Gausian distributions yielded comparable results for the generation of CBD_{max} and CFW values relative to the other methods used in our study (Table 5). When Gausian parameters were expressed using the RGB scheme, roads and feed plots with very low predicted CBD_{bin} values were detected well, appearing black or blue in Fig. 11. Effects of the 1995 wildfire can also be discerned in this figure, appearing as a brown-orange color to the east of the prescribed burn strip.

4. Discussion

We used equations developed by Duveneck and Patterson (2007) to calculate crown fuel weight and canopy bulk density values from biometric measurements made in field plots. The range of DBH and heights of trees harvested by Duveneck and Patterson (2007) to produce predictive equations encompassed the range of trees measured in our field plots. We then calibrated two independent LiDAR systems to canopy fuel characteristics measured in the field plots. We used this information to map canopy fuels in three 9 km^2 areas dominated by pitch pine in the Pinelands of New Jersey. Estimates of CBD and CFW are commonly used throughout the fire management and research communities (e.g., Scott and Reinhardt, 2001), but have not been previously estimated for the Pinelands.

We first compared the two independent LiDAR systems to understand how differences between sensors (e.g., sensor type, acquisition heights) affected our ability to detect canopy fuels estimated from biometric measurements. While the use of scanning LiDAR to estimate canopy fuels facilitates large-spatial scale estimates and the production of landscape level maps of canopy fuels, the more mobile upward sensing profiling LiDAR system can provide immediate estimates of canopy fuels. Comparisons among sensors can improve the reliability of any future rapid canopy fuel assessments using LiDAR sensors, because sensor responses are already well-characterized. For example, understanding the relationships between a simple upward profiling system and canopy fuel attributes allows for the rapid calibration of a scanning LiDAR acquisition by using the profiling system to "calibrate" the scanning system. Quantifying

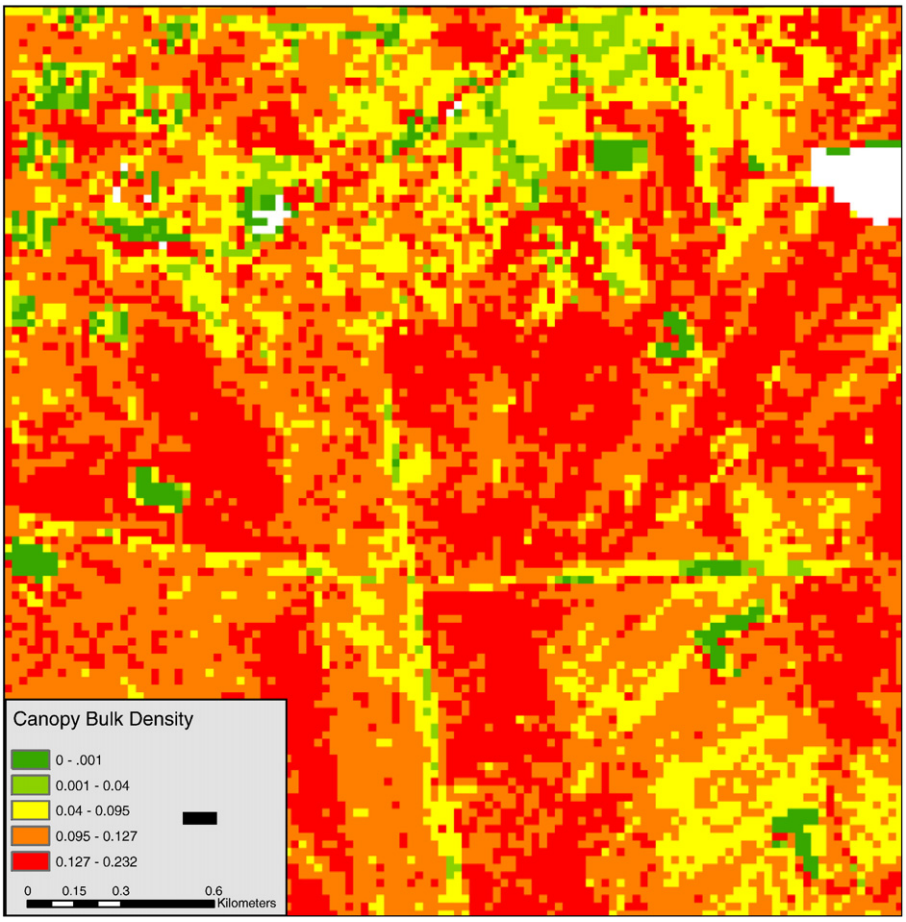

Fig. 6. Map of maximum canopy bulk density (CBD_{max}, kg m^{-3}) predicted with scanning LiDAR data over one of the 9 km^2 study areas at 20 m resolution. Values were calculated from the best-fit stepwise linear regression model in Table 3.

differences among LiDAR systems also may illustrate issues with using sequential LiDAR acquisitions for change detection of canopy fuel parameters.

Table 4
Regression equations to predict canopy bulk density in 1-m canopy layers (CBD_{bin}) using the "all height bins" regression models and the "individual height bins" regression models for selected canopy layers for the profiling and scanning LiDAR systems. The mean PRESS Statistic from leave-one-out cross-validation is reported for the predictive models. Correlations are significant at $P<0.0001$, except where * denotes a significant correlation at $P < 0.05$.

Comparison	*n*	Model	r^2	RMSE	$RMSE_{cv}$
"All height bins" regression models					
Profiling LiDAR	480	$CBD_{bin} = 0.536x + 0.006$	0.83	0.015	0.015
Scanning LiDAR	380	$CBD_{bin} = 0.182x + 0.005$	0.82	0.015	0.015
"Individual height bins" regression models					
Profiling LiDAR					
3-m height	24	$CBD_3 = 0.492x + 0.002$	0.36*	0.006	0.007
8-m height	24	$CBD_8 = 0.418x + 0.230$	0.74	0.023	0.024
13-m height	24	$CBD_{13} = 0.583x + 0.010$	0.82	0.015	0.043
Scanning LiDAR					
3-m height	19	$CBD_3 = 0.075x + 0.007$	0.44	0.005	0.007
8-m height	19	$CBD_8 = 0.583x + 0.009$	0.63	0.027	0.026
13-m height	19	$CBD_{13} = 0.301x - 0.001$	0.99	0.003	0.003
Standard canopy fuel regressions from "all height bins " model					
Profiling LiDAR					
Canopy bulk density	24	$CBD_{max} = 1.021x - 0.003$	0.92	0.011	
Canopy fuel weight	24	$CFW = 1.267x - 0.133$	0.87	0.084	
Scanning LiDAR					
Canopy bulk density	19	$CBD_{max} = 0.841x + 0.021$	0.87	0.012	
Canopy fuel weight	19	$CFW = 0.846x + 0.836$	0.76	0.082	

The relationships between return heights and other LiDAR parameters generated from the upward sensing profiling system and the downward sensing scanning system were all highly significant. However, the slopes for these relationships were not 1:1, and *y*-intercept values were never unity. Mean and maximum return heights (h_{mean} and h_{max}), generated from the upward sensing profiling system, were consistently lower than those calculated from the downward sensing system data for each plot, likely because light

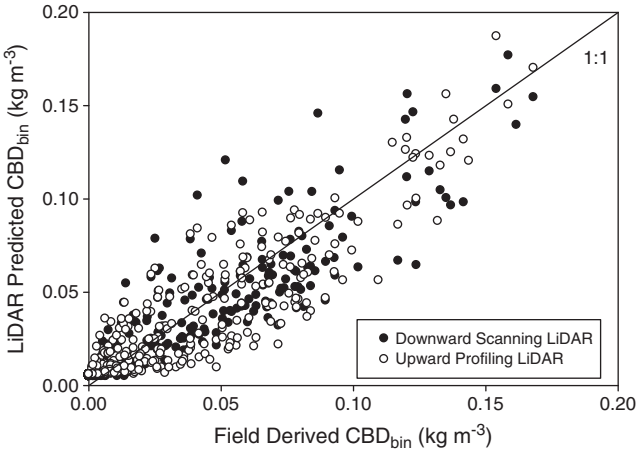

Fig. 7. Predicted values of CBD_{bin} from equations for upward profiling LiDAR (open symbols) and downward scanning LiDAR (closed symbols) in Table 4 plotted against biometric estimates of CBD_{bin} in 1-m layers.

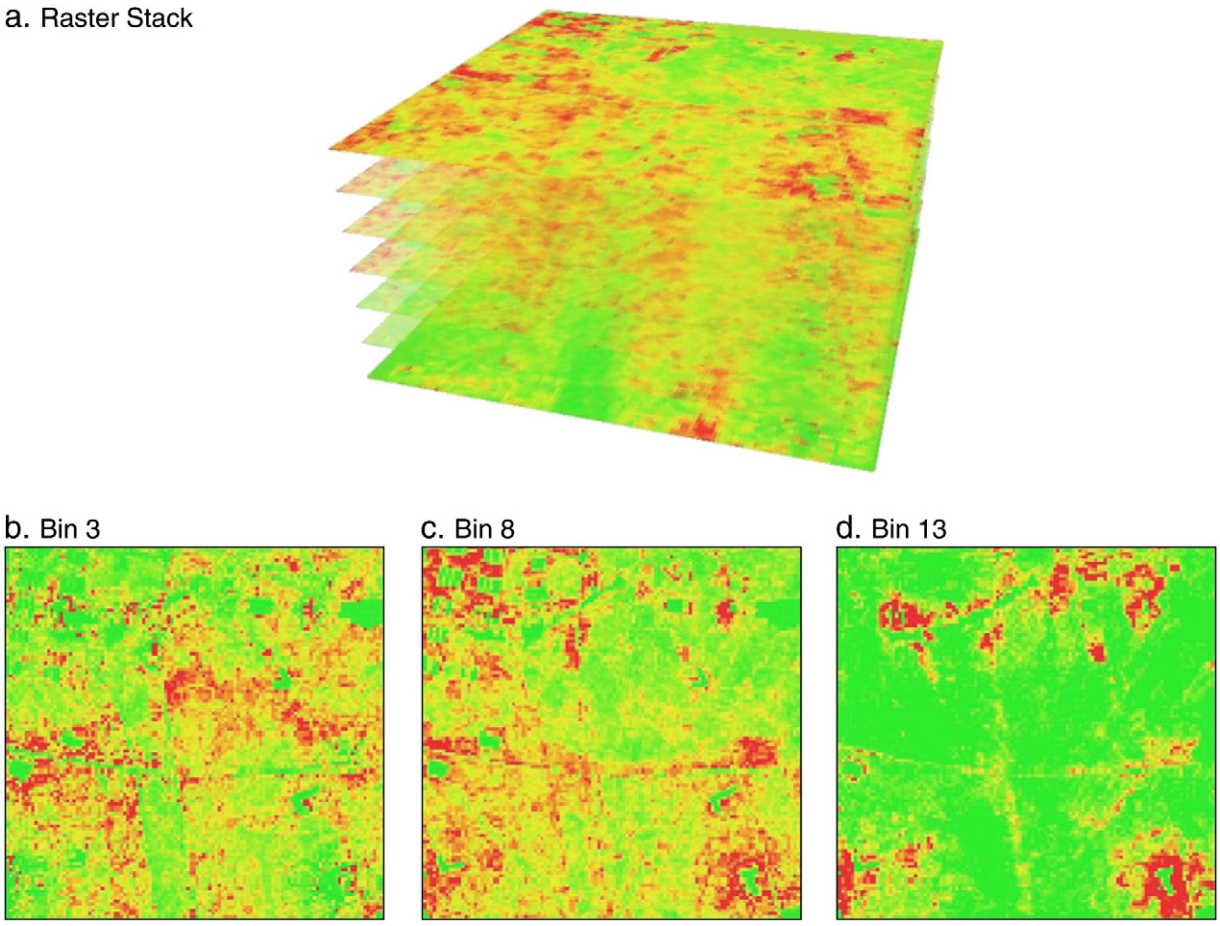

Fig. 8. 9 km^2 maps of canopy bulk density in 1 m canopy layers (CBD_{bin}, kg m^{-3}) at 20 m horizontal resolution predicted using scanning LiDAR data and linear regression models in Table 4. (a) is a raster stack of CBD_{bin} values depicting layers from 1 to 7 m at 1 m vertical resolution. (b)–(d) illustrate CBD bin in three selected height bins (3–4 m height, 8–9 m height, and 13–14 m height from the ground). Pixel color values are relative CBD_{bin} values calculated using regression equations in Table 4, and scale from dark green (0 kg m^{-3}) to red (0.186 kg m^{-3}).

pulses from the two independent LiDAR systems physically encounter the canopy differently (e.g., from above or below). A larger proportion of returns from the upward sensing system encounter foliage and branches lower in the canopy, resulting in a distribution of return heights skewed towards the bottom of the canopy. Similarly, the downward sensing system encounters more foliage and branches at the top of the canopy, which skewed the distribution of returns towards the top of the canopy. The distributions of LiDAR returns may also be affected by the density of points per plot, by the spot size of each return, and by other factors, resulting in different distributions of LiDAR returns. Thus, independent LiDAR acquisitions may not result in 1:1 parameter generation unless repeated under nearly identical circumstances (e.g., instrument, altitude, etc.). Fortunately, our study demonstrates that simple linear regressions may be used to normalize datasets to an acceptable degree.

We first used standard LiDAR-derived parameters (h_{max}, h_{mean}, h_{90}, and D) to predict CBD_{max} and CFW in two dimensions (e.g., Andersen et al., 2005). Both the upward sensing profiling LiDAR and downward sensing scanning LiDAR predicted these variables well. However, when compared to the use of discrete canopy height profiles to calculate CBD_{bin}, a great amount of detail is omitted by expressing canopy fuel loading as only a single CBD_{max} value for each cell. Because these regression models are based primarily on canopy height measurements, the 2-dimensional CBD_{max} may not capture the effects of wildfires on canopy structure, or of prescribed fire or other fuel management activities that may affect sub-canopy and understory fuel loading. In our example near the Cedar Bridge fire tower, the prescribed burn strip had slightly lower values of CBD_{max} than other areas. However, images derived from the CBD_{bin} data indicate much lower fuel loading at 3–4 m height in the burn strip, because repeated prescribed fires have removed some of the understory shrubs and ladder fuels in the sub-canopy (Clark et al., 2009; Skowronski et al., 2007). Thus, parameter-based models can be limited by the use of variables that may not be sensitive to the effects of wildfire, fire management or other disturbances on canopy structure.

The single regression model predicting CBD_{bin} in 1-m canopy layers was highly significant. Some of the variation that was not accounted for by these equations may be explained by the "ideal" nature of the calculated biometric CBD profiles using the Duveneck and Patterson (2007) model. In our analyses, correlation coefficients for between-sensor comparisons were lower, on average, than regression coefficients calculated for the equations relating each LiDAR dataset to the biometric estimates of CBD_{bin} profiles up to 7 m height, and then correlation coefficients were generally greater than regression coefficients above 7 m (as in Fig. 3). Use of regression models likely resulted in the smoothing of some of the vertical variability in canopy structure. These observations suggest that sequential destructive harvest of canopy coupled with concurrent LiDAR acquisitions may be the best approach for developing models to predict CBD_{bin} values from LiDAR data.

Our research demonstrates that LiDAR canopy height profiles can be used to derive estimates of CBD_{bin} that can resolve both horizontal and vertical variability in canopy structure in greater detail than the 2-dimensional CBD_{max} and CFW parameters. This approach can detect the effects of wildfires and prescribed burns on the distribution of CBD in the canopy (Clark et al., 2009; Skowronski et al., 2007). In our

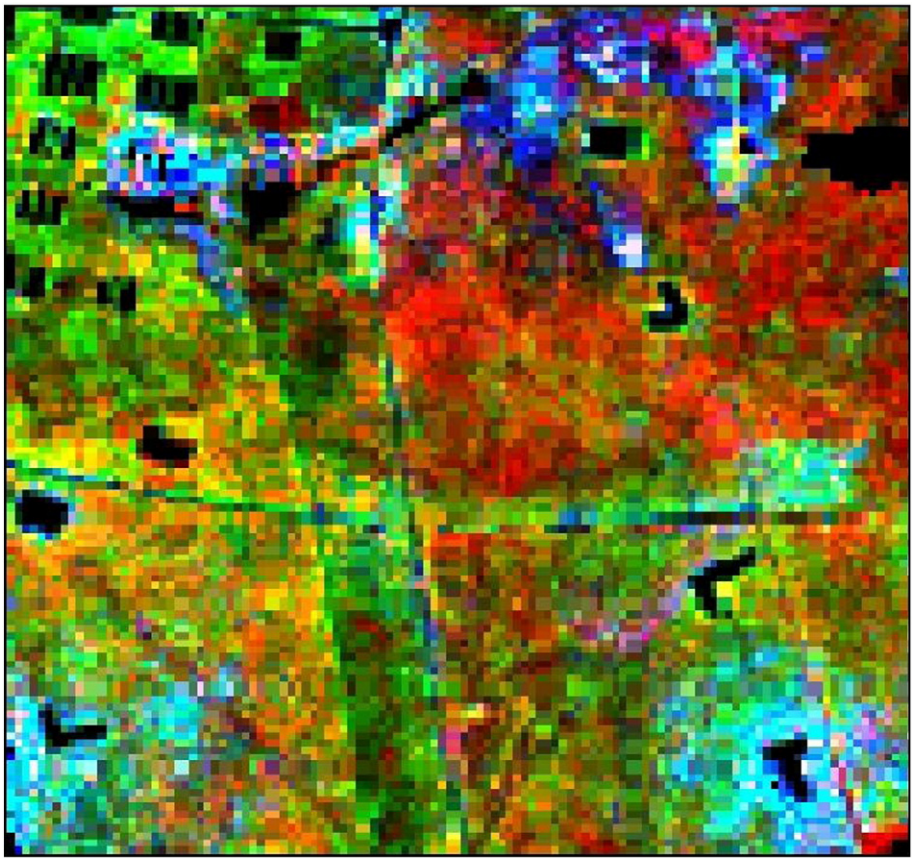

Fig. 9. Red, green, blue (RGB) composites for three bins (red = bin 3, green = bin 8, and blue = bin 13) for the 9 km^2 acquisition near the Cedar Bridge fire tower. The RGB uses a color additive scale scheme with red = bin 3, green = bin 8, and blue = bin 13.

example, the severe wildfire that burned much of the north-eastern portion of the area in 1995 created a mosaic of canopy structure corresponding to fire intensity. Increased amounts of regeneration are clearly visible at 3–4 m height, which 11 years following the wildfire consisted of pitch pine and understory oaks that had recovered to form a dense canopy layer and damaged crowns were still detectable at 8–9 m height. In contrast, an area that is frequently burned as a fuel break using repeated, low-intensity prescribed fires is also visible just to the left of center of the images in Fig. 8. The canopy of this area was not damaged in the 1995 fire, and the overstory remains largely intact at 8–9 m. Only the areas with the tallest canopies contribute to CBD_{bin} values at 13–14 m height in the upper layers of the canopy.

Our results also demonstrate that fitting Gaussian distributions to LiDAR and biometrically derived canopy height profiles allows for a simpler yet meaningful expression of CBD_{bin} for mapping purposes. This method did not perform as well compared to the other methods for deriving the standard canopy fuel parameters CBD_{max} and CFW. Additionally, this method essentially smoothes the data, and valuable information about the vertical distribution of the canopy fuel may be lost; while with the height bin regression approach, differences in

Table 5
Parameters and models for the Gaussian distribution transformation. Data were fit using the function $f(x) = ae^{[-0.5((x-x0)/b)\hat{}2]}$.

Comparison	Parameter	Model	r^2	RMSE	$RMSE_{cv}$
Profiling LiDAR (n = 24)					
	a	$y = 0.318x + 0.036$	0.86	0.012	0.013
	b	$y = 0.528x + 1.328$	0.49	0.183	0.189
	x_0	$y = 1.177x - 0.448$	0.87	0.605	0.622
	CBD_{bin}	$y = 0.941x + 0.002$	0.86		
Scanning LiDAR (n = 19)					
	a	$y = 0.137x + 0.034$	0.81	0.014	0.015
	b	$y = 0.723x + 0.684$	0.80	0.115	0.121
	x_0	$y = 1.16x - 0.511$	0.90	0.545	0.593
	CBD_{bin}	$y = 0.974x + 0.001$	0.92		
Standard canopy fuel derivation					
Profiling LiDAR					
Canopy bulk density		$CBD_{max} = 0.848x + 0.013$	0.88		
Canopy fuel weight		$CFW = 0768x - 0.1.01$	0.86		
Scanning LiDAR					
Canopy bulk density		$CBD_{max} = 0.7868x + 0.020$	0.81		
Canopy fuel weight		$CFW = 0.818 + 0.097$	0.82		

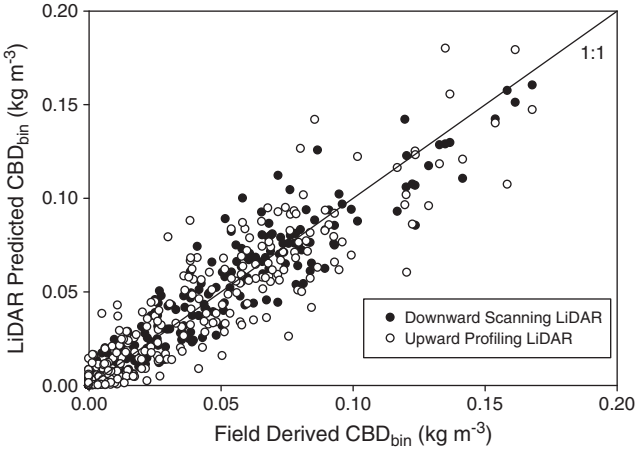

Fig. 10. Field derived CBD_{bin} values plotted against LiDAR predicted CBD_{bin} values. Predictions were made by applying Gaussian distribution transformations to each LiDAR dataset as shown in Table 5.

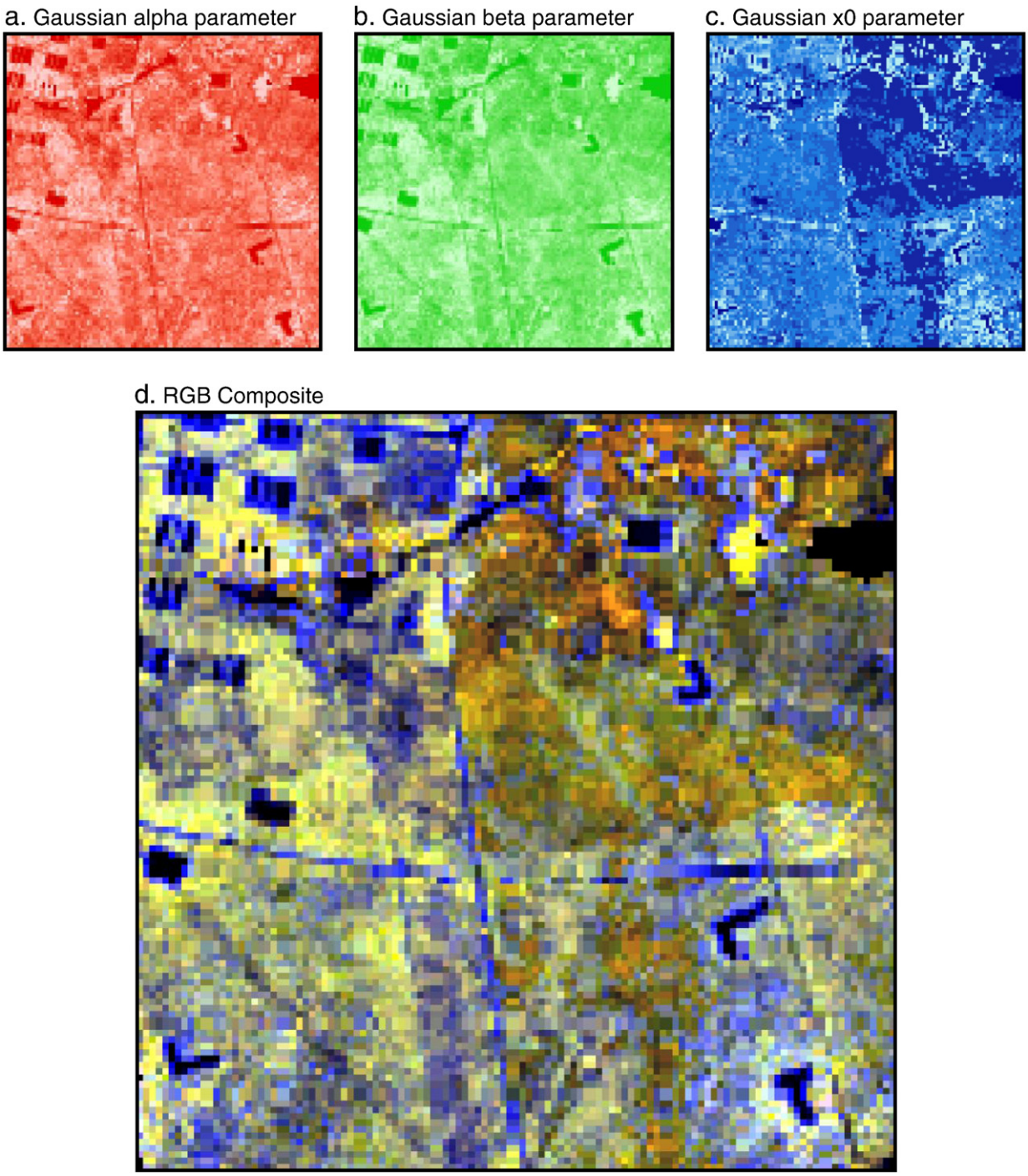

Fig. 11. 9 km^2 maps of three Gaussian parameters (a, b, x_0) and a RGB composite image for one of the three scanning LiDAR extents. The RGB display utilizes a color additive scale scheme with red = a, green = b, and blue = x_0.

individual height bins are maintained for analysis. However, because three parameters are derived from the dataset to characterize the CHP, rather than 20 or more individual bins, it is much easier to display data visually and may simplify otherwise extraneous information. Thus, Gaussian distribution analysis may provide a simple index for analyzing the distribution of canopy fuels, although it may not be the most intuitive method for analyzing spatial variability in canopy fuel loading.

Each of the approaches employed here are advantageous in specific situations, and each has limitations. The expression of the canopy fuel load parameters CFW and CBD_{max} using LiDAR data makes use of standard LiDAR parameters, which are easily derived from a number of commercial data processing packages, and can be used as inputs for existing 2-dimensional wildfire spread models. Estimates of CFW and CBD_{max} provide detail on canopy fuels at the landscape scale, but do not provide information on vertical fuel loading. LiDAR CHP derived estimates of CBD_{bin} provide detailed assessments of three-dimensional canopy structure and fuel loading at the landscape scale, but are much more computationally intensive. Additionally, interpretation of these raster-stacks can be problematic because of the sheer amount of data, and difficulty displaying these data visually without resorting to some type of classification scheme. Finally, the Gaussian distribution (or other similar distribution analyses), though shown to adequately fit the CHPs here, may prove to over-smooth the CHP data and valuable

information may be lost. However, the 3-parameter distribution does show some promise at helping to visualize complex forest structural variability, in a simple RGB environment.

Although we used LiDAR-derived CHPs to predict quantitative CBD_{bin} values, absolute CBD estimates may not be necessary for all fire management assessments, where a relative scale would provide managers with similar information. However, for some applications, such as finer-scale parameter estimation for the next generation of fire behavior models, the calibration of LiDAR data to field data to predict actual three-dimensional CBD values will provide invaluable information.

5. Conclusions

Our study demonstrates that LiDAR data can be used to generate accurate, three-dimensional representations of canopy structure and fuel loading at high spatial resolution by linking 1-m canopy height profiles to predictive calculators derived from forest census plots. This approach provides much more spatially explicit three-dimensional information compared to two-dimensional CFW and CBD_{max} estimates of canopy fuels. Quantification of vertical structure of the canopy is of importance to wildland fire managers, who are interested in managing the landscape for the reduction of ladder or transitional fuels that facilitate the spread of fire into the canopy. Further, this forest structural information is vital for the development of the next generation of wildfire spread models which will simulate fire behavior in three dimensions, unlike the current two-dimensional spread models.

References

Alexander, M. E., Cruz, M. G., & Lopes, A. M. G. (2006). CFIS: A software tool for simulating crown fire initiation and spread. *Forest Ecology and Management*, *234*, S133.

Andersen, H. E., McGaughey, R. J., & Reutebuch, S. E. (2005). Estimating forest canopy fuel parameters using LiDAR data. *Remote Sensing of Environment*, *94*, 441—449.

Clark, K. L., Skowronski, N. S., Hom, J. L., Duveneck, M. J., Pan, Y., Van Tuy, S., Cole, J., Patterson, M., & Maurer, S. (2009). Decision support tools to improve the effectiveness of hazardous fuel reduction treatments in the New Jersey Pine Barrens. *International Journal of Wildland Fire*, *18*, 268—277.

Duveneck, M. J., & Patterson, W. A. (2007). Characterizing canopy fuels to predict fire behavior in pine stands. *Northern Journal of Applied Forestry*, *24*, 65—70.

Finney, M. A. (2004). *FARSITE: Fire Area Simulator—model development and evaluation. Res. Pap. RMRS-RP-4.*Ogden, UT: U.S. Department of Agriculture, Forest Service, Rocky Mountain Research Station 47 pp.

Keane, R. E., Garner, J. L., Schmidt, K. M., Long, D. G., Menakis, J. P., & Finney, M. A. (1998). *Development of input spatial data layers for the FARSITE fire growth model for the Selway-Bitterroot Wilderness complex, USA. Gen. Tech. Rep. RMRS-GTR-3*. Ogden, UT: U.S. Department of Agriculture, Forest Service, Rocky Mountain research Station 66 pp.

Keane, R. E., Mincemoyer, S. A., Schmidt, K. M., Menakis, J. P., Long, D. G., & Garner, J. L. (2000). *Mapping vegetation and fuels for fire management on the Gila National Forest Complex. Gen. Tech. Rep. RMRS-GTR-46.*Ogden, UT: U.S. Department of Agriculture, Forest Service, Rocky Mountain research Station 126 pp.

Keane, R. E., Reinhardt, E. D., Scott, J., Gray, K., & Reardon, J. (2005). Estimating forest canopy bulk density using six indirect methods. *Canadian Journal of Forest Research*, *35*, 724—739.

Lathrop, R. G., & Kaplan, M. B. (2004). *New Jersey land use/land cover update to year 2000-2001*. New Jersey Department of Environmental Protection 35 pp.

McCormick, J., & Jones, L. (1973). *The Pine Barrens: Vegetation Geography. Research Report Vol. 3.*: New Jersey State Museum 76 pp.

Mell, W. E., Manzello, S. L., & Maranghides, A. (2006). Numerical Modeling of Fire Spread through Trees and Shrubs. In D. X. (Ed.), *Proceeding of the 5th International Conference on Forest Fire Research, 27-30 November 2006, Figueira da Foz, Portugal*. Amsterdam, The Netherlands: Elsevier B.V. CD-ROM. 13 pp.

Mutlu, M., Popescu, S. C., Stripling, C., & Spencer, T. (2008). Mapping surface fuel models using LiDAR and multispectral data fusion for fire behavior. *Remote Sensing of Environment*, *112*, 274—285.

Myers, R. H. (1990). *Classical and modern regression with applications. The Duxbury advanced series in statistics and decision science* (pp. 171—178). Boston: PWS-Kent 370.

Parker, G. G., Harding, D. J., & Berger, M. L. (2004). A portable LiDAR system for rapid determination of forest canopy structure. *Journal of Applied Ecology*, *41*, 755—767.

Parker, G. G., Harmon, M. E., Lefsky, M. A., Chen, J., Van Pelt, R., Weis, S. B., Thomas, S. C., Winner, W. E., Shaw, D. C., & Frankling, J. F. (2004). Three-dimensional structure of an Old-growth *Pseudo-Tsuga* canopy and it implications for radiation balance, microclimate, and gas exchange. *Ecosystems*, *7*, 440—453.

Popescu, S. C., Wynne, R. H., & Nelson, R. F. (2003). Measuring individual tree crown diameter with lidar and assessing its influence on estimating forest volume and biomass. *Canadian Journal of Remote Sensing*, *5*, 564—577.

Popescu, S. C., & Zhao, K. (2008). A voxel-based lidar method for estimating crown base height for deciduous and pine trees. *Remote Sensing of Environment*, *112*, 767—781.

Riaño, D., Chuvieco, E., Condes, S., Gonzalez-Matesanz, J., & Ustin, S. L. (2004). Generation of crown bulk density for *Pinus sylvestris* L. from lidar. *Remote Sensing of Environment*, *92*, 345—352.

Scott, J. H. (1999). NEXUS: A system for assessing crown fire hazard. *Fire Management Notes*, *59*(2), 21—24.

Scott, J. H., & Burgan, R. E. (2005). *Standard fire behavior fuel models: A comprehensive set for use with Rothermel's surface fire spread model. Gen. Tech. Rep. RMRS-GTR-153.* Fort Collins, CO: U.S. Department of Agriculture, Forest Service, Rocky Mountain research Station 72 pp.

Scott, J. H., & Reinhardt, E. D. (2001). *Assessing crown fire potential by linking models of surface and crown fire behavior. Research paper RMRS-RP-29.* Fort Collins, CO: U.S. Department of Agriculture, Forest Service, Rocky Mountain research Station 59 pp.

Skowronski, N. S., Clark, K. L., Nelson, R., Hom, J., & Patterson, M. (2007). Remotely sensed measurements of forest structure and fuel loads in the Pinelands of New Jersey. *Remote Sensing of Environment*, *108*, 123—129.

Stoker, J. (2009). Volumetric visualization of multiple-return LiDAR data: Using voxels. *Photogrammetric Engineering and Remote Sensing*, *75*, 109—112.

van Wagner, C. E. (1977). Conditions for the start and spread of crown fire. *Canadian Journal of Forest Research*, *26*, 23—34.